# Detection of Water Ice on 2060 Chiron


Michael J. Foster, Simon F. Green, Neil McBride

*Unit for Space Sciences & Astrophysics, School of Physical Sciences,*

*University of Kent, Canterbury, CT2 7NR, UK*

and

John K. Davies

*Joint Astronomy Centre, 660 N A'ohoku Pl., Hilo, Hawaii, 96720, USA*


August 13, 1999


Number of pages (inc Figs. and Tables): 11

Figures: 2

Tables: 0

Keywords. Chiron, Centaurs, Spectroscopy

Proposed Running Head. Detection of Water Ice on 2060 Chiron.



Correspondence and proofs to:

M.J. Foster

Unit for Space Sciences & Astrophysics

School of Physical Sciences

University of Kent

Canterbury, CT2 7NR, UK

**We present a reflectance spectrum of 2060 Chiron over the wavelength range 1.6–2.2 $\mu$m. The two-micron water ice absorption feature seen in several other Centaurs at $\lambda$=2.03 $\mu$m is identified at the five percent level below the continuum.**

## 1 INTRODUCTION

The Centaurs are minor planets in unstable orbits with semi-major axes between those of Jupiter and Neptune. Dynamical evidence suggests that the Centaurs have migrated inwards from the Kuiper Belt and that similar objects may provide the short period comet population (e.g., Morbidelli *et al.* 1995; Malhotra 1996; Stern and Campins 1996). 2060 Chiron, discovered in 1977 and initially classified as a minor planet (Kowal *et al.* 1979) currently has a 51 year period with a perihelion distance of 8.46 AU and an eccentricity of 0.38. It has a radius of approximately 90 km (Altenhoff and Stumpff 1995; Campins *et al.* 1994) and is a highly unusual object in that it has been observed to be active at distances greater than 12 AU (Hartmann *et al.* 1990). How this activity is driven is not fully understood since the sublimation of water ice which is responsible for the activity of comets in the inner solar system (<3 A.U.) would not occur at such large heliocentric distances. Rather, volatiles such as CO or $CO_2$ are thought to play a crucial role. For example CO drives the activity in comet Hale-Bopp at 5–6 A.U. (Biver *et al.* 1997; Jewitt *et al.* 1996). In an activity model proposed by Prialnik *et al.* (1995), the outburst seen on 2060 Chiron is explained by a combination of energy released by the crystallisation of amorphous water ice and the release of trapped CO from a porous matrix of both amorphous and crystalline ice.

If it is the case that the Centaurs evolve into short period comets, one would expect water ice to be a major constituent. Water ice has been detected on the Centaur 1997 $CU_{26}$ (Brown *et al.* 1998; Brown *et al.* 1999; McBride *et al.* 1999) via infrared absorption features at 1.52 $\mu$m and

2.03 $\mu$m. Water ice has also been seen on 5145 Pholus (Cruikshank *et al.* 1998). Previous IR spectral observations of Chiron have to date been interpreted as featureless and neutral, similar to a C-type asteroid. Luu *et al.* (1994) report a flat featureless spectrum over the 1.6–2.4 $\mu$m waveband.

In this paper we present a 1.6–2.2 $\mu$m spectrum of Chiron in which an absorption feature is seen at around 2 $\mu$m.

## 2 OBSERVATIONS AND DATA REDUCTION

The infrared spectrum of Chiron was obtained with the Cooled Grating Spectrometer (CGS4), on the UK Infrared Telescope UKIRT, Mauna Kea, Hawaii. The spectrometer was configured with its 40 line mm$^{-1}$ grating and its long focal length camera providing a spectral range of 0.64 $\mu$m per grating setting at a resolution of approximately 700. A slit width of 2 pixels ($\sim$1.2 arcsec) was adopted. The seeing was approximately 2.5 pixels ($\sim$1.5 arcsec). The spectra were obtained on 1998 April 24 from 9:26 UT to 10:40 UT over an airmass range of 1.36 to 1.23. At this time Chiron was at a heliocentric distance 8.933 A.U. and a geocentric distance of 7.949 A.U.

To provide good sky subtraction Chiron was nodded up and down the slit, giving a positive and negative beam pair. A total of 35 pairs were taken, each having a total exposure of 100 seconds. However, upon reduction of the data it was noted that the slit had not been perfectly aligned with the direction of the nod, resulting in the object not being centred correctly in the negative beam. We therefore discarded the negative beam data which were of low signal to noise. This resulted in a total exposure time on the object of 1750 seconds.

The instrument's optics result in a curved spectrum which was then straightened in software, by using the signal from a bright star to measure the distortion across the image. The data were resampled and the distortion removed. The rows containing the target spectrum were extracted and wavelength calibrated using the arc lines from the internal calibration lamp.

The G4V star BS5657 was observed at a similar airmass (1.44) to Chiron and used to remove the effects of telluric absorption and to allow the reflectance spectrum to be produced directly. A second star BS3510 (G1V) was also observed to assess the effects of not using an exact solar analogue. Both stars were also observed at a number of different airmasses during the night to evaluate the effect of atmospheric extinction at different wavelengths.

## 3 RESULTS

Fig. 1a and 1b show the 'raw' spectra of Chiron and the two comparison stars. Fig. 1c shows the resulting relative reflectance spectrum of Chiron derived using the star BS5657 and normalised to 1 over the region 2.1–2.2 $\mu$m. Fig. 2a shows the Chiron relative reflectance spectrum after having had an 8-fold binning applied to it. A running mean was not used as this can create artificial features of width equal to the bin size. Fig. 2b shows the spectrum with 16-fold binning applied to it. The error bars shown in the figures are the calculated statistical errors from the number of photons detected. Points that are in regions of less than 50% atmospheric transmission are shown as open circles. The effect of atmospheric absorption is apparent in the 1.8–1.9 $\mu$m region where the data are particularly noisy.

A broad absorption feature can clearly be seen in Fig. 2 centred around 2 $\mu$m with a depth of approximately 5%. Examination of the 'raw' spectra in Fig. 1 show that although the 2 $\mu$m absorption feature occurs in an atmospheric absorption region, the broad 2 $\mu$m absorption seen in Fig. 2 is much wider than the atmospheric feature and there is nothing to indicate that it may be false. Inspection of Fig. 1 indicates that the detailed atmospheric characteristics have been removed successfully. Indeed the data appear 'well behaved' and the atmospheric conditions throughout the observations appeared stable (this is borne out by considering sub-sets of the observations; we find no variation between the subsets).

The absorption feature present is associated with water ice as seen in comet Hale-Bopp (Davies *et al.* 1997) and in 1997 $CU_{26}$ (Brown *et al.* 1998; Brown*et al.* 1999; McBride *et al.* 1999).

It is not possible to detect the presence of the 1.65 $\mu$m feature associated with crystalline ice, although a slight slope is observed in the spectrum here. The overlaid curve in Fig. 2b is the result a spatially distributed mixture of 20% water ice (spectrum taken from Cruikshank *et al.* 1998) combined with 80% spectrally neutral material.

Water ice has also been seen on Pholus (Cruikshank *et al.* 1998) although Pholus displays a number of other unusual spectral features (e.g., Davies *et al.* 1993; Luu *et al.* 1994) not seen in Chiron. Overall the water feature in Chiron is weaker than that seen in 1997 $CU_{26}$ which was also observed on the same night (McBride *et al.* 1999), and would have been difficult to detect at the signal to noise of the previous observations by Luu *et al.* (1994).

Interestingly, there is also a narrow absorption at 2.15 $\mu$m (see Fig. 2). Although this coincides with the stellar Br$\gamma$ absorption line, it does not appear to be simply a consequence of poor stellar subtraction since, (i) it is significantly broader than the stellar line, (ii) the Br$\gamma$ feature is cancelled if we divide our standard star spectrum by another standard star observed at the same airmass (iii) other stellar lines (including Brackett lines at 1.74 and 1.68 $\mu$m) are well corrected, (iv) no such feature is observed in the reflectance spectrum of 1997 $CU_{26}$ taken on the same night (McBride *et al.* 1999).

# 4 DISCUSSION

Chiron was in a low activity phase in 1996 (Lazzaro *et al.* 1996) and observations on April 6th 1998 showed a barely perceptable coma (K. Meech, personal communication). We therefore estimate a contribution from the coma at less than 20%. It is therefore highly unlikely than water ice grains in the coma could solely account for a feature at the 5% level.

The observed highly reddened colours of some Centaurs and Kuiper Belt Objects have been interpreted as evidence for an irradiation mantle caused by cosmic ray bombardment over the lifetime of the solar system. The diversity (or bimodality) in colours (Luu and Jewitt 1996; Green *et al.* 1997; Davies *et al.* 1998; Jewitt and Luu 1998; Romanishin and Tegler 1998) is believed to be the result of removal of the irradiated material exposing pristine ices beneath, or resurfacing by these ices. The mechanisms may be impact related or due to endogenic 'cometary' activity. Since both the most red and blue (*i.e.* the most primitive and most processed?) Centaurs, Pholus and Chiron, both exhibit a water ice feature, and the strongest feature observed so far is for an intermediate object (1997 $CU_{26}$), then it appears that the water ice feature is not a good diagnostic of the degree of processing of the surface. Although we expect water to be a dominant component in all these objects, only a small amount of impurity is required to mask the spectral features. Perhaps then the observed features are related to deposited surface frosts from a modest amount of impact generated vapour, rather than the exposed subsurface material itself.


## ACKNOWLEDGEMENTS

UKIRT is operated by the Joint Astronomy Centre, on behalf of the UK Particle Physics and Astronomy Research Council (PPARC). Image processing and data reduction were performed using the STARLINK network and software. STARLINK is funded by PPARC.


## REFERENCES


Altenhoff, W.J. and P. Stumpff 1995. Size estimate of "asteroid" 2060 Chiron from 250 GHz measurements, *Astron. Astrophys.* **293**, L41–L42.

Brown M.E. and C.D. Koresko 1999. Detection of Water Ice on the Centaur 1997 $CU_{26}$, *Astrophys. J. Letters*, in press.

Brown R.H., D.P. Cruikshank, Y. Pendleton and G.J. Veeder 1998. Identification of Water Ice on the Centaur 1997 $CU_{26}$. *Science* **280**, 1430–1432.

Biver N., D. Bockelee-Morvan, P. Colom, J. Crovisier, J.K. Davies, W.R.F Dent, D. Despois, E. Gerard, E. Lellouch, H. Rauer, R. Moreno and G. Paubert 1997. Evolution of the Outgassing of Comet Hale-Bopp (C/1995 O1) from Radio Observations. *Science* **275**, 1915-1918.

Campins H., C.M. Telesco, D.J. Osip, G.H. Rieke and B. Schultz 1994. The Colour Temperature of 2060 Chiron — A Warm Small Nucleus. *Astron. J.* **108**, 2318–2322.

Cruikshank D.P., T.L. Roush, M.J. Bartholomew, T.R. Geballe, Y.J. Pendleton, S.M. White, J.F. Bell, J.K. Davies, T.C. Owen, C. de Bergh, D.J. Tholen, M.P. Bernstein, R.H. Brown, K.A. Tryka, C.M. Dalleore 1998. The Composition of Centaur 5145 Pholus. *Icarus* **135** 389-407.

Davies, J.K., T.L. Roush, D.P. Cruikshank, M.J. Bartholomew, T.R. Geballe, T. Owen and C. de Bergh 1997. Detection of Water Ice in Comet Hale-Bopp. *Icarus* **127**, 238–245.

Davies, J.K., N. McBride, S.L. Ellison, S.F. Green and D.R. Ballantyne 1998. Infrared Photometry of Six Centaurs. *Icarus* **134**, 213–227.

Green S.F., N. McBride, D O'Ceallaigh, A. Fitzsimmons, I.P. Williams and M.J. Irwin 1997. Surface Reflectance Properties of Distant Solar Bodies. *Mon. Not. R. astr. Soc.* **290**, 186–192.

Hartmann W.K., D.J. Tholen, K.J. Meech and D.P. Cruikshank 1990. Chiron: Colorimetry and Cometary Behaviour. *Icarus* **83**, 1–15.

Kowal C.T., W. Liller and B.G. Marsden 1979. The Discovery and Orbit of (2060) Chiron. In *Dynamics of the Solar System* (R.L. Duncombe Ed), pp. 245, Kluwer, Dordrecht.

Jewitt, D. and J. Luu 1998. Optical-Infrared Spectral Diversity in the Kuiper Belt. *Astron. J.* **115** 1667–1670.

Jewitt D., M. Senay and H. Matthews 1996. Observations of Carbon Monoxide in Comet Hale-Bopp. *Science* **271**, 1110–1113.

Lazzaro D., M.A. Florczak, A. Betzlier, O.C. Winter, S.M. Giuliatti-Winter, C.A. Angeli, D.W. Foryta 1996. 2060 Chiron back to a minimum of brightness. *Planet. Space Sci.* **44**, 1547–1550.

Luu J., D. Jewitt and E. Cloutis 1994. Near infrared spectroscopy of primitive solar system objects. *Icarus* **109**, 133–144.

Luu J. and D. Jewitt 1996. Color Diversity Among the Centaurs and Kuiper Belt Objects. *Astron. J.* **112**, 2310–2318.

Malhotra R. 1996. The Phase Structure Near Neptune Resonances in the Kuiper Belt. *Astron. J.* **111**, 504–516.

McBride N., J.K. Davies, S.F. Green and M.J. Foster 1999. Optical and Infrared Observations of the Centaur 1997 $CU_{26}$. *Mon. Not. R. astr. Soc.*, in press.

Morbidelli A., F. Thomas and M. Moons 1995. The Resonance Structure of the Kuiper Belt and the Dynamics of the First Five Trans-Neptunian Objects. *Icarus* **118**, 322–340.

Prialnik D., N. Brosch and D. Ianovici 1995. Modelling the Activity of 2060-Chiron. *Mon. Not. R. Astr. Soc.* **276**, 1148–1154.

Stern A. and H. Campins 1996. Chiron and the Centaurs: Escapees from the Kuiper Belt. *Nature* **382**, 507–510.

Tegler S.C. and W. Romanishin 1998. Two Distinct Populations of Kuiper Belt Objects. *Nature* **392**, 49–51.

## Figure captions

**Figure 1.** Spectra of 2060 Chiron and comparison stars. (a) The raw spectrum of 2060 Chiron. (b) The raw spectrum of star BS5657 (G4V), which is used to produce the relative reflectance spectrum of Chiron. (c) The relative reflectance spectrum of 2060 Chiron (Fig. a divided by Fig. b) presented here unbinned.

**Figure 2.** Relative reflectance spectra of 2060 Chiron. Here, the spectrum presented in Fig. 1c is binned to improve signal to noise. Note that running mean smoothing has not been applied in order to avoid creating artificial features of width equal to the bin size. Points that are in regions of less than 50% atmospheric transmission are shown as open circles. (a) The spectrum having had 8-fold binning applied. (a) The spectrum having had 16-fold binning applied. The overlaid curve in Fig. 2b is the result a spatially distributed mixture of 20% water ice (spectrum taken from Cruikshank *et al.* 1998) combined with 80% spectrally neutral material.

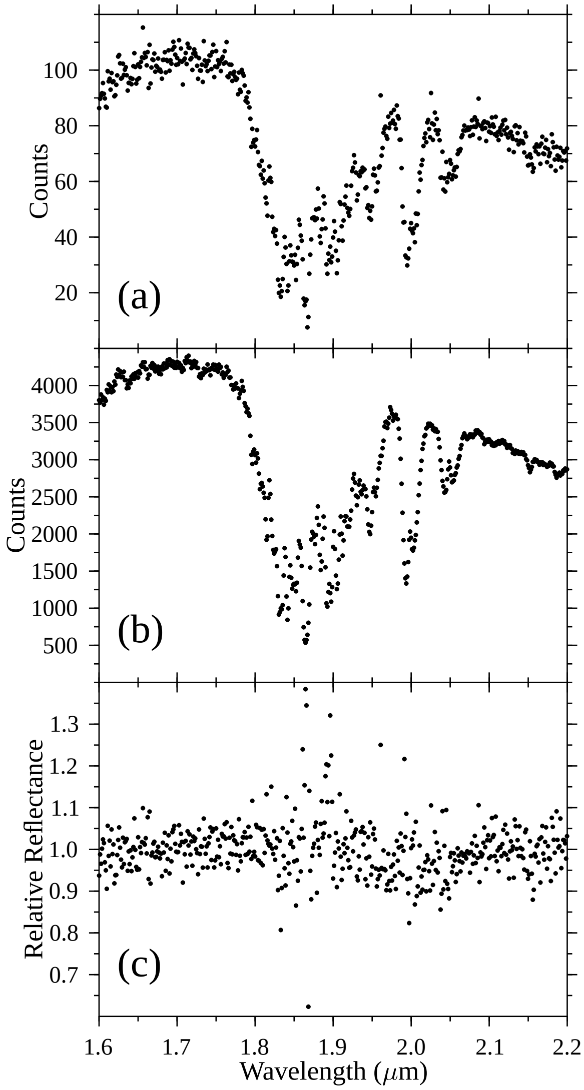

(a)
(b)
(c)
Counts
Counts
Relative Reflectance
Wavelength ($\mu$m)
1.6
1.7
1.8
1.9
2.0
2.1
2.2


Figure 1:

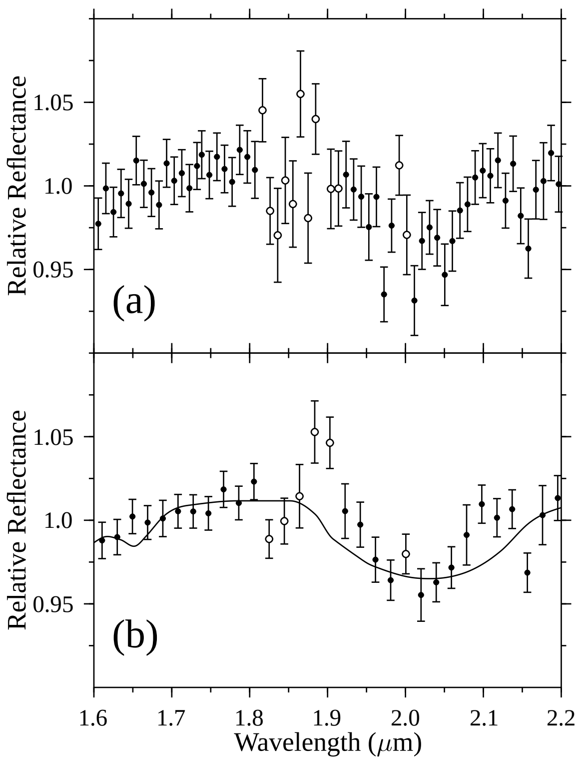
Relative Reflectance
1.05
1.0
0.95
(a)
Relative Reflectance
1.05
1.0
0.95
(b)
1.6
1.7
1.8
1.9
2.0
2.1
2.2
Wavelength (μm)

Figure 2: